Title
Parkinsonism Driven by Antipsychotics Originates from Dopaminergic Control of Striatal Cholinergic Interneurons.

Journal
Neuron, 91(1)

ISSN
0896-6273

Authors
Kharkwal, Geetika
Brami-Cherrier, Karen
Lizardi-Ortiz, José E
et al.

Publication Date
2016-07-01

DOI
10.1016/j.neuron.2016.06.014

Peer reviewed

HHS Public Access

Author manuscript

Neuron. Author manuscript; available in PMC 2017 July 06.

Published in final edited form as:

Neuron. 2016 July 6; 91(1): 67–78. doi:10.1016/j.neuron.2016.06.014.

Parkinsonism driven by antipsychotics originates from dopaminergic control of striatal cholinergic interneurons

Geetika Kharkwal[1,*], **Karen Brami-Cherrier**[1,*], **José E. Lizardi-Ortiz**[2], **Alexandra B. Nelson**[3,4], **Maria Ramos**[1], **Daniel Del Barrio**[1], **David Sulzer**[2], **Anatol C. Kreitzer**[3], and **Emiliana Borrelli**[1]

[1]Department of Microbiology & Molecular Genetics, U904 INSERM/UCI, University of California, Irvine, CA 92697

[2]Departments of Neurology and Pharmacology, Columbia University, New York, NY 10032, USA

[3]The Gladstone Institutes, San Francisco, CA 94158

[4]Department of Neurology, University of California, San Francisco, CA 94158

Summary

Typical antipsychotics can cause disabling side effects. Specifically, antagonism of D2R signaling by the typical antipsychotic haloperidol induces parkinsonism in humans and catalepsy in rodents. Striatal dopamine D2 receptors (D2R) are major regulators of motor activity through their signaling on striatal projection neurons and interneurons. We show that D2R signaling on cholinergic interneurons contributes to an in vitro pause in firing of these otherwise tonically active neurons and to the striatal dopamine/acetylcholine balance. The selective ablation of D2R from cholinergic neurons allows discrimination between the motor-reducing and cataleptic effects of antipsychotics. The cataleptic effect of antipsychotics is triggered by blockade of D2R on cholinergic interneurons and the consequent increase of acetylcholine signaling on striatal projection neurons. These studies illuminate the critical role of D2R-mediated signaling in regulating the activity of striatal cholinergic interneurons and the mechanisms of typical antipsychotic side effects.

Introduction

Aberrant dopaminergic control of striatal circuits contributes to human neurological and psychiatric disorders (Crittenden and Graybiel, 2011). In the striatum, medium spiny

Correspondence to: Emiliana Borrelli.

*Equal contribution

Authors contribution

M.R. generated ChI-D2RKO mice, G.K, K.B.-C. conceived, performed and analyzed behavioral and cellular experiments with D.D.B.; J.E.L-O and D.S. conceived, performed and interpreted CV studies while A.B.N. and A.C.K. electrophysiological experiments. EB designed the study, interpreted results, and wrote the manuscript with K.B.-C.

neurons (MSNs) are the most abundant neurons and the only output of this structure. MSNs are thus critical elements in striatum-regulated functions such as the control of movement and motivation. Neuronal networks formed by extra-striatal and intra-striatal inputs finely regulate MSN activity (Gittis and Kreitzer, 2012). Dopamine (DA) is a major modulator of MSN activity. Indeed, loss of DA neurons in Parkinson's disease impairs voluntary movements and other DA-dependent functions (Gittis and Kreitzer, 2012; Surmeier, 2013). However, DA regulation of striatal neurons is not restricted to MSNs but also extends to striatal cholinergic interneurons (ChIs) that, despite their low number, appear to regulate striatal microcircuits (Aosaki et al., 2010; Nelson et al., 2014; Witten et al., 2010).

ChIs, also known as tonically active neurons (Aosaki et al., 1994a; Apicella, 2002), integrate excitatory inputs from the thalamus and cortex with inputs from DA and GABA neurons, leading to regulation of MSN outputs (Chuhma et al., 2014; Surmeier and Graybiel, 2012). Previous studies have revealed the presence of a reciprocal relationship between DA neurons and ChIs. Acetylcholine (ACh) stimulates dopaminergic neurons activity and the release of DA and GABA (Cachope et al., 2012; Nelson et al., 2014; Threlfell et al., 2012); in return DA inhibits or stimulates ChI activity and ACh release, depending on whether it acts through D2 receptors (D2R) (Straub et al., 2014) or D5R (Aosaki et al., 2010; Centonze et al., 2003; Lester et al., 2010). The synergism between DA and ACh has important consequences for the activity of MSNs, which compose the direct and indirect pathways (Gerfen and Surmeier, 2011). Importantly, the activity of MSNs is modulated by muscarinic receptors (Threlfell et al., 2010; Threlfell and Cragg, 2011). These findings suggest the presence of a tight DA-regulated interplay between MSN and ChI activity.

D2Rs are central regulators of the DA/ACh interaction since both DAergic neurons and ChIs express these receptors. D2R activation inhibits neuronal activity and the release of DA (Anzalone et al., 2012) and ACh (DeBoer and Abercrombie, 1996). Interestingly, DA bursts have been shown to induce pauses in the tonic activity of striatal ChIs and to trigger a transient suppression of cortical inputs on the MSNs within the indirect pathway (Ding et al., 2010; Shen et al., 2007; Thorn and Graybiel, 2010). This class of MSNs (Gerfen and Surmeier, 2011) expresses D2R (Delle Donne et al., 1997) whose signaling modulates the striato-thalamic-cortical circuit (Surmeier et al., 2009; Tozzi et al., 2011). Importantly, antipsychotics used in the treatment of schizophrenia and other psychiatric disorders block D2R signaling. In humans blockade of D2Rs with the typical antipsychotic haloperidol has debilitating side-effects known as extrapyramidal symptoms which include dystonia, parkinsonism and tardive dyskinesia. In rodents, haloperidol induces catalepsy, the inability to initiate voluntary movements. To date, the mechanisms underlying the side effects of antipsychotics are not fully understood.

Given the complex interplay between neuronal types and DA signaling together with the heterogeneous D2R distribution, the functional contribution of D2R in specific striatal neurons has been difficult to address, especially in the very sparse ChIs (Tepper and Bolam, 2004). To solve this question of both conceptual and biomedical importance, we have generated mice with cell type-specific ablation of D2R in ChIs (hereafter named ChI-D2RKO mice). Importantly, the ChIs of ChI-D2RKO mice show significantly shorter pauses in firing after intrastriatal stimulation, corroborating a critical role of D2R signaling in

generating the pause in vitro. Strikingly, the catalepsy induced by haloperidol is suppressed in ChI-D2RKO mice. These results underline the importance of D2R signaling in ChIs in the control of motor function and will be valuable towards the development of alternative pharmacological strategies.

Results

Ablation of D2Rs from cholinergic interneurons

D2Rs are expressed on many striatal cell types, as well as on the axon terminals of many striatal inputs (De Mei et al., 2009). Pharmacological tools cannot target D2R in specific cell-types in vivo, preventing the elucidation of the role of D2R signaling in ChIs. We sought to address this issue of fundamental biomedical importance by generating ChI-specific D2RKO (ChI-D2RKO) mice and analyzing how their ablation would influence behavioral and cellular parameters.

D2R floxed mice (Anzalone et al., 2012) were crossed with heterozygous transgenic mice expressing Cre recombinase under the control of the choline acetyl transferase (ChAT) promoter (Gong et al., 2003)(Figure S1A). Southern blot analyses confirmed the presence of D2R floxed alleles as well as of Cre recombinase in the genome of ChI-D2RKO mice (Figure S1B). ChI-D2RKO mice have normal weight, size, and fertility as compared to WT littermates. Since ChIs constitute 1–2% of total striatal cell population (Tepper and Bolam, 2004) we assessed the full deletion of D2R in these interneurons by fluorescent activated cell sorter (FACS) experiments using ChAT antibodies and DAPI as marker of nuclei (Figure 1A) followed by qRT-PCR of RNAs prepared from sorted ChAT-positive and negative neurons from animals of both genotypes. These experiments confirmed the absence of D2R specific transcripts only in the ChIs of ChI-D2RKO as compared to WT mice ($p<0.05$ Figure 1B) while in ChAT-negative neurons both genotypes showed similar levels of D2R expression ($p>0.05$).

ACh is involved in the control of DA release from the dopaminergic terminals via activation of nicotinic (Rice et al., 2011) and muscarinic receptors (Foster et al., 2014); abnormal ChI function in ChI-D2RKO mice might alter evoked DA release. We thus compared the evoked DA overflow in the dorsal striatum by performing cyclic voltammetry (CV) in WT and ChI-D2RKO brain slices. CV data analysis revealed that a similar level of DA overflow was evoked in both genotypes in response to single pulse electrical stimulation ($n= 30$/group; $p= 0.35$; Figure 1C left panel); instead 20 Hz pulse trains elicited a significant increase of DA overflow in ChI-D2RKO as compared to WT mice ($p=0.02$; Figure 1C right panel). We then tested D2 autoreceptor mediated inhibition of DA overflow in ChI-D2RKO mice. When incubated with 0.5 μM of the D2R agonist quinpirole, ChI-D2RKO slices displayed quinpirole-mediated reduction in DA overflow, an effect still present but to a lesser extent in WT littermates ($p< 0.0001$; Figure 1D). Thus, absence of control of D2R on ChIs affects DA release.

Reduced ChI “pause” in the absence of D2R

To determine whether deletion of D2Rs from ChIs might generate changes in their intrinsic or synaptic properties, we performed both cell-attached and whole-cell patch-clamp recordings of ChI in coronal brain slices from adult ChI-D2RKO and WT littermates (Figure 2A). At 33°C, ChIs of both genotypes fired spontaneously in cell-attached mode (Figure 2B), as previously reported in rodents (Bennett and Wilson, 1999). The observed rates were not significantly different (p=0.69; Figure 2B, right panel). ChIs from both genotypes showed typical intrinsic properties in whole-cell current-clamp mode (Figure 2C), which did not differ between WT and ChI-D2RKO slices (Table S1), suggesting that the ionic conductances responsible for tonic firing and responses to hyperpolarizing and depolarizing stimuli are not grossly disrupted in ChI-D2RKO mice. Several studies have described a “pause” in the firing of ChIs *in vivo* in response to salient or reward-predictive stimuli (Aosaki et al., 1994b). The synaptic and cellular mechanisms are not entirely understood, although DA is involved (Aosaki et al., 1994b; Straub et al., 2014). To examine whether the pause may be disrupted in ChI-D2RKO mice, we modified a previously published in vitro protocol for eliciting a pause in the spontaneous firing of cholinergic interneurons (Ding et al., 2010), using intrastriatal rather than thalamic stimulation. This 50 Hz, 5 pulse protocol is expected to activate both cortical and thalamic afferents to ChIs, as well as local DA inputs, and elicited an immediate excitatory response followed by a pause response in WT ChIs (Figure 2D, left panel). We quantified the ChI pause in two ways: (1) the difference between the observed first post-stimulation interspike interval (ISI) and the expected ISI based on the baseline firing rate, and (2) the ratio of the observed ISI and the expected ISI. In WT slices, the pause was 278+/−105 msec in duration (n=15 neurons), and the ISI ratio was 1.72 +/− 0.38 (n=15 neurons). These values are somewhat lower than previously observed (Ding et al., 2010) and may be related to the use of intrastriatal rather than thalamic stimulation, as well as the use of a train of 5, rather than 10 stimuli. Prior work has suggested that the pause in vivo and in vitro is dopamine-mediated, but a pause has also been observed in response to stimulation of midbrain GABAergic neurons (Brown et al., 2012). To determine whether the in vitro pause response we elicited was dopamine-dependent, GABA-dependent, or both, we applied the GABA receptor antagonist picrotoxin and the D2R antagonist sulpiride sequentially to WT neurons. Only the latter caused a marked reduction in the duration of the pause (Figure S2), suggesting that in our recordings, dopamine was the major contributor. In ChI-D2RKO mice, the pause response to such stimulation was also markedly reduced as compared to WT mice (Figure 2D, right panel), measuring 25 +/− 38 msec (Figure 2E; n=24; p=0.013 in comparison to WT) with an ISI ratio of 1.13 +/− 0.05 (Figure 2F; n=24; p= 0.012 in comparison to WT). These findings demonstrate that a dopamine-dependent in vitro pause response, which bears some similarities to that seen in vivo in response to reward or reward-predictive cues, is markedly reduced In ChI-D2RKO mice.

D2R signaling in cholinergic interneurons modulates motor behavior

Next we assessed the impact of D2R removal from ChIs on motor activity under basal conditions. Forward locomotion was recorded in ChI-D2RKO mice and WT littermates during the light/dark cycle using an actimetric rack (Figure S3A) or during 1h in a novel home cage (NHC) (Figure S3B). Both genotypes had similar locomotor (NHC: n=14/genotype; p>0.05; Actimetric: n=8/genotype; p>0.05) and rearing activity in the NHC

(n=11; p>0.05, Figure S3B). These results indicate that loss of D2R on ChIs does not lead to major motor deficits in ChI-D2RKO mice analyzed in basic conditions.

DA acting through either D2R (inhibitory) or D5R (stimulatory) modulates the activity of ChIs; at the same time, DA excites MSNs of the direct pathway through D1R signaling while inhibits MSNs of the indirect pathway through D2R (Gerfen and Surmeier, 2011). ACh signaling has the opposite effect than DA on the direct and indirect pathways (Aosaki et al., 2010; Shen et al., 2008; Surmeier, 2013). In addition, ACh stimulates DA release from dopaminergic neurons (Cachope et al., 2012; Threlfell et al., 2012). To test the hypothesis that ChIs contribute to the regulation of motor activity upon DA stimulation, we analyzed ChI-D2RKO motor behavior after pharmacological challenge using agonists and antagonists for both D1Rs and D2Rs.

In the mouse, quinpirole, a D2R agonist, depresses motor activity (Usiello et al., 2000). This effect depend on the presynaptic inhibition of dopamine release (Usiello et al., 2000) but also from the heterosynaptic inhibition of the release of other neurotransmitters from striatal (ChI, MSN) as well as extrinsic neurons (Anzalone et al., 2012; Bamford et al., 2004; DeBoer and Abercrombie, 1996). Systemic administration of quinpirole dose-dependently decreased motor activity in mice of both genotypes (Figure 3A). However, quinpirole more efficiently reduced motor activity in ChI-D2RKO mice than in WT siblings. This difference hints to a more efficient quinpirole-mediated inhibition of DA levels in ChI-D2RKO mice particularly evident at the lowest concentration used. It has been shown that ACh regulates DA release through stimulation of nicotinic receptors on DA terminals (Rice et al., 2011). The knockout of D2Rs in ChIs by preventing the DA-mediated inhibition of ACh release might result into desensitization of nicotinic receptors on DA neurons with a consequent decrease of DA levels (Threlfell et al., 2010).

Stimulation of D1-like receptors was achieved using SKF 81297. This compound stimulates striatal D1Rs expressed by MSNs and D5Rs by ChIs (Aosaki et al., 2010) and increases motor activity (Usiello et al., 2000). SKF81297 administration, analyzed during 1 h in NHC, dose-dependently induced forward locomotion in mice of both genotypes (Figure 3B). Nevertheless, in response to SKF 81297 there was a clear trend toward a lower induction of motor activity in ChI-D2RKO as compared to WT mice. This result suggests that SKF81297 less efficiently activate D1R signaling on the MSNs of ChI-D2RKO mice. Importantly, SKF81297 also stimulates D1-like receptors (D5R) on ChIs inducing ACh release (Abercrombie and DeBoer, 1997; DeBoer and Abercrombie, 1996). Thus, a reasonable explanation for these results is that loss of the D2R-mediated inhibition of ACh in ChI-D2RKO mice further promotes SKF81297-mediated ACh release. Stimulation of the inhibitory M4 receptors on $D1R^{+}$-MSNs counterbalances the direct activation by SKF 81297 of D1Rs on these same neurons inhibiting their activity and consequently locomotion. In support of these results, analyses of the D1R- and cAMP-dependent phosphorylation of GluR1 (Ser^{845} residue) (Snyder et al., 2000) by SKF 81297 paralleled behavioral data showing lower induction of GluR1 phosphorylation in ChI-D2RKO striatal extracts as compared to WT (Figure S3C). Altogether, the behavioral responses of ChI-D2RKO mice to D1- and D2-like agonists suggest the presence of finely tuned control mechanisms of motor activity involving the dopaminergic regulation of ChIs.

D2R signaling in cholinergic interneurons partition motor and cataleptic responses

Blockade of either D1-like or D2-like receptors greatly reduces forward locomotion and induces catalepsy (Usiello et al., 2000). SCH23390, a D1-like antagonist, and haloperidol a D2-like antagonist, dose-dependently reduced forward locomotion in mice of both genotypes (Figure 3C, 3D and S3D).

Interestingly, both SCH23390- and haloperidol-induced catalepsy as measured with the bar test was markedly different between genotypes. SCH 23390-induced catalepsy was much less prominent in ChI-D2RKO than in WT mice ($p<0.0001$; Figure 3E). Even more surprising, while haloperidol produces catalepsy in control mice, it does not in ChI-D2RKO mice at all doses tested ($p<0.0001$; Figure 3F) as well as at different time points after administration ($p<0.01$; Figure S3E). These results indicate that catalepsy arises from the acute blockade of dopamine receptors not only on MSNs but more importantly on ChIs. Interestingly, D2Rs control ACh release (Abercrombie and DeBoer, 1997) and scopolamine, a non-selective muscarinic antagonist, has been reported to attenuate haloperidol-induced catalepsy (Fink-Jensen et al., 2011). Thus, our experiments suggest that the D2R-mediated control of striatal ChI physiology critically modulates catalepsy. In agreement, scopolamine reversed the effect of haloperidol on catalepsy in WT mice (Figure S3F) while, as expected, has no effect on ChI-D2RKO mice.

Haloperidol-induced cellular responses are blunted in ChI-D2RKO mice

We next explored the intracellular effects of loss of D2R signaling in ChI-D2RKO mice. We used a marker of intracellular signaling activation, the phosphorylation of the ribosomal protein S6 (rpS6) on $Ser^{235/236}$ and $Ser^{240/244}$ residues (Knight et al., 2012). Phosphorylation (P) of these residues in the striatum in response to haloperidol has been linked to the activation of the cAMP ($Ser^{235/236}$) (Valjent et al., 2011) and mTorc 1 ($Ser^{240/244}$) signaling pathways (Bonito-Oliva et al., 2013). Furthermore, phosphorylation of $Ser^{240/244}$ has been proven to reflect activation of striatal ChIs (Bertran-Gonzalez et al., 2012). We used antibodies directed against P-rpS6-$Ser^{240/244}$ together with choline acetyltransferase (ChAT) to investigate activation of intracellular signaling in ChIs in response to haloperidol in the dorsolateral striatum (DLS) (Gerfen, 1992) of WT and ChI-D2RKO mice 1h after haloperidol administration (Figure 4A). Saline treatment did not alter the percentage of rpS6-$Ser^{240/244}$ phosphorylation in ChIs or of fluorescence intensity/cell in the DLS of WT and ChI-D2RKO sections (Figure 4A and 4B). In agreement with previous reports, haloperidol administration induced P-rpS6-$Ser^{240/244}$ in the vast majority of ChIs as well as the fluorescence intensity/cell in the WT DLS (Figure 4A and B left and right). Strikingly, the induction of rpS6-$Ser^{240/244}$ phosphorylation in response to haloperidol was completely abolished in the ChIs of ChI-D2RKOs ($p<0.0001$; Figure 4A and B left and right).

In striatal $D2R^{+}$-MSNs, haloperidol induces the phosphorylation of rpS6 on $Ser^{235/236}$ (Valjent et al., 2011). To explore the possibility that dampening of rpS6 phosphorylation after haloperidol in ChI-D2RKO cholinergic interneurons might also indirectly affect signaling to rpS6 in $D2R^{+}$-MSNs, we performed double immunofluorescence analyses using antibodies specific for P-rpS6-$Ser^{235/236}$ and for the adenosine A_{2A} receptor, a marker of

D2R$^+$-MSNs. Haloperidol treatment resulted into potent 8–9-fold induction of the number of D2R$^+$-MSNs showing a stronger rpS6-Ser$^{235/236}$ phosphorylation/cell in the WT DLS ($p<0.0001$, Figure 4C and 4D). Interestingly, in ChI-D2RKO striata the number of P-rpS6 positive D2R$^+$-MSNs was less than half that of WT mice ($p<0.0001$; Figure 4D left and right) and the fluorescence intensity/cell did not increase with respect to saline treated mice, although it was sensibly higher in saline conditions in ChI-D2RKO as compared to WT D2R$^+$-MSNs ($p<0.0001$; Figure 4D). These results show that a smaller population of D2R$^+$-MSNs responds to haloperidol in ChI-D2RKO as compared to WT mice, and that these events correlate with the dampened signaling to rpS6-Ser$^{240/244}$ in ChIs.

Acetylcholine signaling mediates the cataleptic effect of haloperidol

ChIs of the DLS express M2 and M4 muscarinic autoreceptors that inhibit ACh release (Threlfell et al., 2010). In addition, ACh release is also negatively regulated by dopamine through activation of D2Rs. Absence of D2R in the ChIs removes the dopaminergic inhibition over ACh release, which in specific conditions (i.e. haloperidol treatment) might lead to a sustained ACh-mediated activation of muscarinic autoreceptors and consequent reduction of ACh release. Thus we hypothesized that absence of catalepsy in ChI-D2RKO mice might be explained by a reduced cholinergic signaling in the striatum. To test this hypothesis we blocked ACh degradation using donepezil, an acetylcholinesterase inhibitor, which increases striatal ACh levels (Karvat and Kimchi, 2014) and tested the behavioral and cellular effects on haloperidol-treated ChI-D2RKO and WT littermates.

Importantly, no changes in the expression of M2, M4 or of M1 muscarinic receptors were detected between WT and ChI-D2RKO mice (Figure S4A). Mice were given combined treatments with donepezil (0.3 or 1mg/kg) or saline 15 minutes prior to haloperidol (1mg/kg) or saline administration. Locomotion as well as catalepsy were measured 1h after the last injection (Figure 5A, 5B). Single haloperidol or donepezil administration significantly affected motor activity in WT and ChI-D2RKO mice (treatment: $p<0.0001$; Figure 5A); when combined, the two drugs did not reduce further motor activity as compared to haloperidol in both genotypes. Donepezil by itself did not induce catalepsy (Figure 5B). Importantly, however, donepezil administration prior to haloperidol dose-dependently restored catalepsy ($p<0.0001$ both doses vs saline) in ChI-D2RKO mice reaching WT levels at the highest dose (Figure 5B). Donepezil did not increase haloperidol-induced catalepsy in WT mice (Figure 5B). These findings point to ACh signaling being involved in the side-effects of haloperidol through blockade of D2Rs located on cholinergic interneurons.

To determine whether the restoration of haloperidol-induced catalepsy in donepezil-treated ChI-D2RKO mice was accompanied by normalization of haloperidol-induced cellular responses, we assessed the induction of rpS6 phosphorylation in simple or combined treatments. Interestingly, donepezil by itself induced rpS6-Ser$^{240/244}$ phosphorylation in a similar percentage of ChIs ($p<0.05$) and fluorescence intensity/cell ($p<0.0001$) in both genotypes (Figure 5C). Combined donepezil and haloperidol treatments did not further increase the percentage or intensity/cell as compared to donepezil alone (Figure 5C). These results support our hypothesis of a diminished ACh level in ChI-D2RKO.

Importantly, at the intracellular level donepezil in WT and ChI-D2RKO mice induced rpS6-Ser$^{235/236}$ phosphorylation in a similar number of D2R^{+}-MSNs in both genotypes ($p<0.05$; Figure 5D left). In addition, combined with haloperidol, donepezil had a cumulative effect on both the number of induced cells ($p<0.05$–0.01; Figure 5D left) and on fluorescence intensity/cell in both genotypes ($p<0.0001$, Figure 5D right). These results indicate that ACh is directly involved in the stimulation of ChIs and D2R^{+}-MSNs signaling that leads to rpS6 phosphorylation and suggest that catalepsy is induced by the increased release of ACh from ChIs and activation of muscarinic receptors on MSNs in the presence of a D2R antagonist. In line with these findings, scopolamine (1mg/kg) decreased haloperidol-induced (1mg/kg) phosphorylation of rpS6-Ser$^{240/244}$ in ChIs (Figure S4B, S4C) and of Ser$^{235/236}$ in the D2R^{+}-MSNs ($p<0.05$, Figure S4D) in WT sections, while having no effects in ChI-D2RKO cells ($p>0.05$, Figure S4C).

Typical vs atypical antipsychotics

Haloperidol, the prototype of typical antipsychotics, induces catalepsy, while atypical antipsychotics such as clozapine do not (Vauquelin et al., 2012). Clozapine has partial agonist (M2/M4) as well as antagonist (M1) effects on muscarinic receptors (Michal et al., 1999; Seeman, 2014; Zeng et al., 1997). We hypothesized that absence of clozapine-induced catalepsy might depend on the pharmacological properties of this compound for muscarinic receptors. In this case scenario we would expect clozapine to have similar effects on rpS6 phosphorylation in WT and ChI-D2RKO mice. We firstly assessed that clozapine at 1 and 3mg/kg was equally able to reduce horizontal motor activity in both WT and ChI-D2RKO mice (Figure S5). Interestingly, the phosphorylation pattern of rpS6 in ChI-D2RKO slices in response to clozapine administration (Figure 6A–6D) was completely different from that of haloperidol (Figure 4A–4D). Indeed, clozapine induced P-rpS6-Ser$^{240/244}$ in a similar percentage of ChIs and to equal intensity in both genotypes ($p<0.01$ Figure 6A and 6B left anrd right), while it did not significantly induce rpS6-Ser$^{235/236}$ phosphorylation in D2R^{+}-MSNs independent from the genotype ($p>0.05$; Figure 6C and 6D left and right). These results are consistent with our hypothesis that the absence of clozapine-induced catalepsy is due to its heterogeneous affinity for multiple receptors including muscarinic receptors (Michal et al., 1999; Zeng et al., 1997; Seeman, 2014). Indeed, clozapine was able to reduce the extent of rpS6-Ser$^{235/236}$ phosphorylation induced by donepezil in D2R^{+}-MSNs ($p<0.05$; Figure 6F left and right), likely antagonizing M1 receptors on these cells (Seeman, 2014), but not on ChIs ($p<0.05$; Figure 6E left and right) through the partial agonist activity.

These results suggest that typical antipsychotics induce catalepsy through selective ACh stimulation of D2R^{+}-MSNs. In support of this conclusion, we performed experiments in which M1 muscarinic receptors were blocked by the specific antagonist N-[3-oxo-3-[4-(4-pyridinyl)-1-piperazinyl]propyl]-2,1,3-benzothiadiazole-4-sulfonamide (VU0255035) (Maltese et al., 2014; Xiang et al., 2012). Administration of VU0255035 (30 and 60mg/kg) 1h after haloperidol (1mg/kg) significantly reduced the time that mice spent immobile during the bar test as compared to haloperidol alone (Figure 7A). The behavioral effect of co-administered haloperidol and VU0255035 was mirrored by the cellular response of D2R^{+}-MSNs to the combined treatment showing the absence of haloperidol-induced phosphorylation of rpS6-Ser$^{235/236}$ in D2R^{+}-MSNs similar to what we obtained using

clozapine (Figure 7B, 7C). Conversely, the combined treatment did not change the phosphorylation of rpS6-Ser$^{240/244}$ in ChIs as compared to haloperidol alone, as expected (Figure S6A, B). Thus, the simultaneous blockade of D2R and M1R abolishes catalepsy; this event is paralleled by the loss of induction of rpS6-Ser$^{235/236}$ phosphorylation in D2R^{+}-MSNs.

Discussion

Cholinergic interneurons are critical elements in the control of striatal circuits (Cachope et al., 2012; Ding et al., 2010; Thorn and Graybiel, 2010; Threlfell et al., 2012; Witten et al., 2010).

ChI-D2RKO mice represent the first mouse model where D2Rs have been specifically and selectively removed from ChIs, thereby providing an excellent system to study the impact of dopamine signaling on these neurons.

It is known that ACh activation of nicotinic receptors on DA neurons results in a high probability of initial DA release, but limits subsequent release by high frequency stimulation (Patel et al., 2012; Zhang and Sulzer, 2004). Our cyclic voltammetry analyses show that loss of D2R on ChIs impairs this finely regulated mechanism. Furthermore, the inhibition of DA overflow by quinpirole, which is completely abolished in the constitutive D2R−/− mouse (Baik et al., 1995; Rouge-Pont et al., 2002), is partly preserved in ChI-D2RKO as well as in all conditional D2R mutants examined so far (Anzalone et al., 2012). Thus, the control of DA release depends on D2R activation on DA neurons themselves, but also on MSNs and cholinergic interneurons.

ChIs are tonically active and pause in coincidence with DA bursts (Goldberg and Reynolds, 2011; Morris et al., 2004) suggesting that DA receptor signaling contributes to the pausing (Aosaki et al., 2010; Apicella, 2002; Schulz and Reynolds, 2013; Straub et al., 2014). We demonstrate that absence of D2R in ChIs reduces the in vitro pause of these neurons, consistent with the idea that D2R on cholinergic interneurons themselves play a critical role in mediating the pause.

An additional implication that emanates from our results relates to the locomotor phenotype. Indeed, ACh signaling in the striatum is known to regulate locomotion through activation of muscarinic and nicotinic receptors located on striatal neurons and afferent fibers (Patel et al., 2012). We demonstrate that loss of D2R signaling on ChIs does not alter baseline movement parameters. Conversely, loss of D2R signaling in ChIs significantly affects motor behavior after challenges with DA agonists or antagonists. Interestingly, behavioral responses to both D1-like (SKF81297) and D2-like (quinpirole) agonists differed between WT and ChI-D2RKO mice. Thus, our findings implicate that ChI-mediated responses gate motor activity through modulation of DA signaling.

A most unexpected finding of this study is that haloperidol, a D2R antagonist and typical antipsychotic, no longer induces catalepsy in ChI-D2RKO mice. Catalepsy in rodents is a model of the extrapyramidal syndrome and of parkinsonisms that follow antipsychotic therapies (Eskow Jaunarajs et al., 2015; Seeman, 2010). The selective, cell-specific D2R

ablation in cholinergic interneurons allowed us to reveal the neuronal mechanisms underlying haloperidol-induced effects. We demonstrate that the motor reducing effect of haloperidol is intact in ChI-D2RKO mice because dependent on blockade of D2Rs on MSNs. Surprisingly, we show that catalepsy is abolished in ChI-D2RKO mice. These results indicate that the side effects of typical antipsychotics depend on blockade of D2Rs on ChIs. The extensive expression pattern of D2Rs on multiple striatal neurons and afferent fibers has previously prevented the identification of this mechanism.

In the absence of D2Rs in ChIs, haloperidol-mediated rpS6-Ser$^{240/244}$ phosphorylation (Bertran-Gonzalez et al., 2012) is eliminated. In parallel, phosphorylation of the rpS6 residue Ser$^{235/236}$ in response to haloperidol in D2R^{+}-MSNs (Bonito-Oliva et al., 2013; Valjent et al., 2011) is greatly reduced in ChI-D2RKO mice as compared to WT littermates. Both the behavioral and cellular responses to haloperidol in ChI-D2RKO are reinstated when haloperidol is co-administered with an inhibitor of ACh degradation (Figure 5). Thus, the catalepsy evoked by haloperidol in WT mice appears to be caused by the acute blockade of D2R not only on MSNs but also on ChIs, causing larger release of ACh and subsequent increase in ACh-mediated signaling in D2R^{+}-MSNs.

Results presented here suggest that the reduced side effects of the atypical antipsychotic clozapine and related compounds likely depend on their affinity for muscarinic receptors. The development of novel antipsychotics targeting D2Rs or the use of existing ones together with modulators of muscarinic receptors (Kruse et al. 2014) might be fruitful pharmacological strategies that could improve antipsychotic therapies.

The present study provides the first direct evidence for the key role of D2R on ChIs in conferring normal striatal functions. It also shows that DA and ACh act in concert to orchestrate finely tuned movements through a feed-forward mechanism involving DA and cholinergic interneurons. This bidirectional mechanism has a strong impact on the MSNs, the major output neurons of the striatum and consequently on movements.

Experimental procedures

Animals

ChI-D2RKO mice were generated by breeding D2R$^{flox\text{-}flox}$ mice (Anzalone et al., 2012) with Tg(ChAT-CRE)24Gsat mice (MMRRC, UC Davis) (Gong et al., 2007; Gong et al., 2003) (see SI). Age matched (8–12 week old) male mice were used for experiments. Protocols were approved by the Institutional Animal Care and Use Committee in accordance to NIH guidelines.

Fluorescence Activated Cell Sorting and qPCR

ChIs were sorted (FACSAriaII/FACSDiva) from striatal cells of ChI-D2RKO and WT mice using ChAT antibodies, RNAs extracted, retrotranscribed and subjected to RT-qPCR using D2R, and GAPDH primers (See SI).

Amperometry, and Cyclic Voltammetry

Experiments were performed on 250μm slices (Schmitz et al., 2002) with some modifications (See SI).

Electrophysiological Characterization of cholinergic interneurons

Recordings on coronal brain slices were made in either the cell-attached or whole-cell current clamp mode to measure spontaneous firing rate and intrinsic excitability, respectively. Pause-response experiments were performed in both modes. The pause response was measured as either the ratio of the first inter-spike interval (ISI) following stimulation versus the average ISI during the baseline period (Ding et al., 2010) ("ISI ratio"), or as the actual pause (ISI between the last action potential during the stimulation period and the next action potential) minus the expected pause (the average ISI in the baseline period) (see SI).

Behavioral Analyses

Locomotor activity in novel home cage (NHC) was recorded (1h) using a videotracking system (Videotrack, Les Ulis). Catalepsy was measured using the bar test (Usiello et al., 2000). Pharmacological treatments were administered in NHC and motor activity recorded as indicated in figure legends; all compounds were from Sigma (St. Louis, MO) (See also SI).

Immunofluorescence analyses

Double immunostainings were performed on vibratome sections (Brami-Cherrier et al., 2005) using either rpS6-$Ser^{240/244}$ or -$Ser^{235/236}$ together with either ChAT or $A_{2A}R$ specific antibodies. Quantifications were performed on confocal images (SP5, Leica) of coronal striatal slices (3 section/animal and 3 brains/genotype/condition). To quantify the number of $D2R^{+}$-MSNs showing the induction of rpS6 phosphorylation, frames of 375×375 μm/image (n=4) were defined and the number of double $A_{2A}R$- and P-rpS6-$Ser^{235\text{-}236}$ positive cells counted. For ChIs, 2 frames of 775×775 μm/image each per coronal striatal section and 10 ChIs/frame were analyzed. Data are expressed as percentage of ChIs showing rpS6-$Ser^{240/244}$ phosphorylation above threshold (see SI) on a total of 10 $ChAT^{+}$ neurons/frame. For quantifications of intensity/cell: ROIs were drawn around individual cells (ChI or MSNs) using LAS-AF software (Leica); mean gray values/cell were obtained and background subtracted.

Statistical Analyses

Data are expressed as mean ± SEM. Data were analyzed by 2-way ANOVA followed by either Bonferroni's post hoc comparisons or Paired two-tailed Student's t-test, as appropriate, using GraphPad Prism 6.00. CV experiments with multiple pulses were analyzed by 2-way ANOVA with repeated measure followed by Bonferroni's post-hoc test. In Figure 1D, F test on nonlinear regression was used. Electrophysiological experiments were analyzed by Student's t-test.

Supplementary Material

Refer to Web version on PubMed Central for supplementary material.

Acknowledgments

These studies were supported from NIH (DA024689; DA033554) and INSERM funds to EB. We acknowledge Dr. Daniela Radl for discussions and N. Hoshi for sharing equipment; S. Nolen, R. Lewis, J. Liu for assistance and V. Scarfone for assistance with FACS experiments and analyses.

References

Abercrombie ED, DeBoer P. Substantia nigra D1 receptors and stimulation of striatal cholinergic interneurons by dopamine: a proposed circuit mechanism. J Neurosci. 1997; 17:8498–8505. [PubMed: 9334422]

Anzalone A, Lizardi-Ortiz JE, Ramos M, De Mei C, Hopf FW, Iaccarino C, Halbout B, Jacobsen J, Kinoshita C, Welter M, et al. Dual control of dopamine synthesis and release by presynaptic and postsynaptic dopamine D2 receptors. J Neurosci. 2012; 32:9023–9034. [PubMed: 22745501]

Aosaki T, Graybiel AM, Kimura M. Effect of the nigrostriatal dopamine system on acquired neural responses in the striatum of behaving monkeys. Science. 1994a; 265:412–415. [PubMed: 8023166]

Aosaki T, Miura M, Suzuki T, Nishimura K, Masuda M. Acetylcholine-dopamine balance hypothesis in the striatum: an update. Geriatrics & gerontology international. 2010; 10(Suppl 1):S148–157. [PubMed: 20590830]

Aosaki T, Tsubokawa H, Ishida A, Watanabe K, Graybiel AM, Kimura M. Responses of tonically active neurons in the primate's striatum undergo systematic changes during behavioral sensorimotor conditioning. J Neurosci. 1994b; 14:3969–3984. [PubMed: 8207500]

Apicella P. Tonically active neurons in the primate striatum and their role in the processing of information about motivationally relevant events. The European journal of neuroscience. 2002; 16:2017–2026. [PubMed: 12473069]

Baik JH, Picetti R, Saiardi A, Thiriet G, Dierich A, Depaulis A, Le Meur M, Borrelli E. Parkinsonian-like locomotor impairment in mice lacking dopamine D2 receptors. Nature. 1995; 377:424–428. [PubMed: 7566118]

Bamford NS, Robinson S, Palmiter RD, Joyce JA, Moore C, Meshul CK. Dopamine modulates release from corticostriatal terminals. J Neurosci. 2004; 24:9541–9552. [PubMed: 15509741]

Bennett BD, Wilson CJ. Spontaneous activity of neostriatal cholinergic interneurons in vitro. J Neurosci. 1999; 19:5586–5596. [PubMed: 10377365]

Bertran-Gonzalez J, Chieng BC, Laurent V, Valjent E, Balleine BW. Striatal cholinergic interneurons display activity-related phosphorylation of ribosomal protein S6. PloS one. 2012; 7:e53195. [PubMed: 23285266]

Bonito-Oliva A, Pallottino S, Bertran-Gonzalez J, Girault JA, Valjent E, Fisone G. Haloperidol promotes mTORC1-dependent phosphorylation of ribosomal protein S6 via dopamine- and cAMP-regulated phosphoprotein of 32 kDa and inhibition of protein phosphatase-1. Neuropharmacology. 2013; 72:197–203. [PubMed: 23643747]

Brami-Cherrier K, Valjent E, Herve D, Darragh J, Corvol JC, Pages C, Arthur SJ, Girault JA, Caboche J. Parsing molecular and behavioral effects of cocaine in mitogen- and stress-activated protein kinase-1-deficient mice. J Neurosci. 2005; 25:11444–11454. [PubMed: 16339038]

Brown MT, Tan KR, O'Connor EC, Nikonenko I, Muller D, Luscher C. Ventral tegmental area GABA projections pause accumbal cholinergic interneurons to enhance associative learning. Nature. 2012; 492:452–456. [PubMed: 23178810]

Cachope R, Mateo Y, Mathur BN, Irving J, Wang HL, Morales M, Lovinger DM, Cheer JF. Selective activation of cholinergic interneurons enhances accumbal phasic dopamine release: setting the tone for reward processing. Cell reports. 2012; 2:33–41. [PubMed: 22840394]

Centonze D, Grande C, Saulle E, Martin AB, Gubellini P, Pavon N, Pisani A, Bernardi G, Moratalla R, Calabresi P. Distinct roles of D1 and D5 dopamine receptors in motor activity and striatal synaptic plasticity. J Neurosci. 2003; 23:8506–8512. [PubMed: 13679419]

Chuhma N, Mingote S, Moore H, Rayport S. Dopamine neurons control striatal cholinergic neurons via regionally heterogeneous dopamine and glutamate signaling. Neuron. 2014; 81:901–912. [PubMed: 24559678]

Crittenden JR, Graybiel AM. Basal Ganglia disorders associated with imbalances in the striatal striosome and matrix compartments. Frontiers in neuroanatomy. 2011; 5:59. [PubMed: 21941467]

De Mei C, Ramos M, Iitaka C, Borrelli E. Getting specialized: presynaptic and postsynaptic dopamine D2 receptors. Current opinion in pharmacology. 2009; 9:53–58. [PubMed: 19138563]

DeBoer P, Abercrombie ED. Physiological release of striatal acetylcholine in vivo: modulation by D1 and D2 dopamine receptor subtypes. The Journal of pharmacology and experimental therapeutics. 1996; 277:775–783. [PubMed: 8627558]

Delle Donne KT, Sesack SR, Pickel VM. Ultrastructural immunocytochemical localization of the dopamine D2 receptor within GABAergic neurons of the rat striatum. Brain Res. 1997; 746:239–255. [PubMed: 9037503]

Ding JB, Guzman JN, Peterson JD, Goldberg JA, Surmeier DJ. Thalamic gating of corticostriatal signaling by cholinergic interneurons. Neuron. 2010; 67:294–307. [PubMed: 20670836]

Eskow Jaunarajs KL, Bonsi P, Chesselet MF, Standaert DG, Pisani A. Striatal cholinergic dysfunction as a unifying theme in the pathophysiology of dystonia. Progress in neurobiology. 2015; 127–128:91–107.

Fink-Jensen A, Schmidt LS, Dencker D, Schulein C, Wess J, Wortwein G, Woldbye DP. Antipsychotic-induced catalepsy is attenuated in mice lacking the M4 muscarinic acetylcholine receptor. European journal of pharmacology. 2011; 656:39–44. [PubMed: 21269601]

Foster DJ, Gentry PR, Lizardi-Ortiz JE, Bridges TM, Wood MR, Niswender CM, Sulzer D, Lindsley CW, Xiang Z, Conn PJ. M5 receptor activation produces opposing physiological outcomes in dopamine neurons depending on the receptor's location. J Neurosci. 2014; 34:3253–3262. [PubMed: 24573284]

Gerfen CR. The neostriatal mosaic: multiple levels of compartmental organization. Trends in neurosciences. 1992; 15:133–139. [PubMed: 1374971]

Gerfen CR, Surmeier DJ. Modulation of striatal projection systems by dopamine. Annual review of neuroscience. 2011; 34:441–466.

Gittis AH, Kreitzer AC. Striatal microcircuitry and movement disorders. Trends in neurosciences. 2012; 35:557–564. [PubMed: 22858522]

Goldberg JA, Reynolds JN. Spontaneous firing and evoked pauses in the tonically active cholinergic interneurons of the striatum. Neuroscience. 2011; 198:27–43. [PubMed: 21925242]

Gong S, Doughty M, Harbaugh CR, Cummins A, Hatten ME, Heintz N, Gerfen CR. Targeting Cre recombinase to specific neuron populations with bacterial artificial chromosome constructs. J Neurosci. 2007; 27:9817–9823. [PubMed: 17855595]

Gong S, Zheng C, Doughty ML, Losos K, Didkovsky N, Schambra UB, Nowak NJ, Joyner A, Leblanc G, Hatten ME, et al. A gene expression atlas of the central nervous system based on bacterial artificial chromosomes. Nature. 2003; 425:917–925. [PubMed: 14586460]

Karvat G, Kimchi T. Acetylcholine elevation relieves cognitive rigidity and social deficiency in a mouse model of autism. Neuropsychopharmacology : official publication of the American College of Neuropsychopharmacology. 2014; 39:831–840. [PubMed: 24096295]

Knight ZA, Tan K, Birsoy K, Schmidt S, Garrison JL, Wysocki RW, Emiliano A, Ekstrand MI, Friedman JM. Molecular profiling of activated neurons by phosphorylated ribosome capture. Cell. 2012; 151:1126–1137. [PubMed: 23178128]

Kruse AC, Kobilka BK, Gautam D, Sexton PM, Christopoulos A, Wess J. Muscarinic acetylcholine receptors: novel opportunities for drug development. Nat Rev Drug Discov. 2014; 13:549–560. [PubMed: 24903776]

Lester DB, Rogers TD, Blaha CD. Acetylcholine-dopamine interactions in the pathophysiology and treatment of CNS disorders. CNS neuroscience & therapeutics. 2010; 16:137–162. [PubMed: 20370804]

Maltese M, Martella G, Madeo G, Fagiolo I, Tassone A, Ponterio G, Sciamanna G, Burbaud P, Conn PJ, Bonsi P, et al. Anticholinergic drugs rescue synaptic plasticity in DYT1 dystonia: role of M1 muscarinic receptors. Mov Disord. 2014; 29:1655–1665. [PubMed: 25195914]

Michal P, Lysikova M, El-Fakahany EE, Tucek S. Clozapine interaction with the M2 and M4 subtypes of muscarinic receptors. European journal of pharmacology. 1999; 376:119–125. [PubMed: 10440097]

Morris G, Arkadir D, Nevet A, Vaadia E, Bergman H. Coincident but distinct messages of midbrain dopamine and striatal tonically active neurons. Neuron. 2004; 43:133–143. [PubMed: 15233923]

Nelson AB, Hammack N, Yang CF, Shah NM, Seal RP, Kreitzer AC. Striatal cholinergic interneurons Drive GABA release from dopamine terminals. Neuron. 2014; 82:63–70. [PubMed: 24613418]

Patel JC, Rossignol E, Rice ME, Machold RP. Opposing regulation of dopaminergic activity and exploratory motor behavior by forebrain and brainstem cholinergic circuits. Nature communications. 2012; 3:1172.

Rice ME, Patel JC, Cragg SJ. Dopamine release in the basal ganglia. Neuroscience. 2011; 198:112–137. [PubMed: 21939738]

Rouge-Pont F, Usiello A, Benoit-Marand M, Gonon F, Piazza PV, Borrelli E. Changes in extracellular dopamine induced by morphine and cocaine: crucial control by D2 receptors. J Neurosci. 2002; 22:3293–3301. [PubMed: 11943831]

Schmitz Y, Schmauss C, Sulzer D. Altered dopamine release and uptake kinetics in mice lacking D2 receptors. J Neurosci. 2002; 22:8002–8009. [PubMed: 12223553]

Schulz JM, Reynolds JN. Pause and rebound: sensory control of cholinergic signaling in the striatum. Trends in neurosciences. 2013; 36:41–50. [PubMed: 23073210]

Seeman P. Dopamine D2 receptors as treatment targets in schizophrenia. Clinical schizophrenia & related psychoses. 2010; 4:56–73. [PubMed: 20643630]

Seeman P. Clozapine, a fast-off-D2 antipsychotic. ACS chemical neuroscience. 2014; 5:24–29. [PubMed: 24219174]

Shen W, Flajolet M, Greengard P, Surmeier DJ. Dichotomous dopaminergic control of striatal synaptic plasticity. Science. 2008; 321:848–851. [PubMed: 18687967]

Shen W, Tian X, Day M, Ulrich S, Tkatch T, Nathanson NM, Surmeier DJ. Cholinergic modulation of Kir2 channels selectively elevates dendritic excitability in striatopallidal neurons. Nature neuroscience. 2007; 10:1458–1466. [PubMed: 17906621]

Snyder GL, Allen PB, Fienberg AA, Valle CG, Huganir RL, Nairn AC, Greengard P. Regulation of phosphorylation of the GluR1 AMPA receptor in the neostriatum by dopamine and psychostimulants in vivo. J Neurosci. 2000; 20:4480–4488. [PubMed: 10844017]

Straub C, Tritsch NX, Hagan NA, Gu C, Sabatini BL. Multiphasic modulation of cholinergic interneurons by nigrostriatal afferents. J Neurosci. 2014; 34:8557–8569. [PubMed: 24948810]

Sur C, Mallorga PJ, Wittmann M, Jacobson MA, Pascarella D, Williams JB, Brandish PE, Pettibone DJ, Scolnick EM, Conn PJ. N-desmethylclozapine, an allosteric agonist at muscarinic 1 receptor, potentiates N-methyl-D-aspartate receptor activity. Proceedings of the National Academy of Sciences of the United States of America. 2003; 100:13674–13679. [PubMed: 14595031]

Surmeier DJ. Neuroscience: To go or not to go. Nature. 2013; 494:178–179. [PubMed: 23354047]

Surmeier DJ, Graybiel AM. A feud that wasn't: acetylcholine evokes dopamine release in the striatum. Neuron. 2012; 75:1–3. [PubMed: 22794253]

Surmeier DJ, Plotkin J, Shen W. Dopamine and synaptic plasticity in dorsal striatal circuits controlling action selection. Current opinion in neurobiology. 2009; 19:621–628. [PubMed: 19896832]

Tepper JM, Bolam JP. Functional diversity and specificity of neostriatal interneurons. Current opinion in neurobiology. 2004; 14:685–692. [PubMed: 15582369]

Thorn CA, Graybiel AM. Pausing to regroup: thalamic gating of cortico-basal ganglia networks. Neuron. 2010; 67:175–178. [PubMed: 20670826]

Threlfell S, Clements MA, Khodai T, Pienaar IS, Exley R, Wess J, Cragg SJ. Striatal muscarinic receptors promote activity dependence of dopamine transmission via distinct receptor subtypes on cholinergic interneurons in ventral versus dorsal striatum. J Neurosci. 2010; 30:3398–3408. [PubMed: 20203199]

Threlfell S, Cragg SJ. Dopamine signaling in dorsal versus ventral striatum: the dynamic role of cholinergic interneurons. Frontiers in systems neuroscience. 2011; 5:11. [PubMed: 21427783]

Threlfell S, Lalic T, Platt NJ, Jennings KA, Deisseroth K, Cragg SJ. Striatal dopamine release is triggered by synchronized activity in cholinergic interneurons. Neuron. 2012; 75:58–64. [PubMed: 22794260]

Tozzi A, de Iure A, Di Filippo M, Tantucci M, Costa C, Borsini F, Ghiglieri V, Giampa C, Fusco FR, Picconi B, et al. The distinct role of medium spiny neurons and cholinergic interneurons in the D(2)/A(2)A receptor interaction in the striatum: implications for Parkinson's disease. J Neurosci. 2011; 31:1850–1862. [PubMed: 21289195]

Usiello A, Baik JH, Rouge-Pont F, Picetti R, Dierich A, LeMeur M, Piazza PV, Borrelli E. Distinct functions of the two isoforms of dopamine D2 receptors. Nature. 2000; 408:199–203. [PubMed: 11089973]

Valjent E, Bertran-Gonzalez J, Bowling H, Lopez S, Santini E, Matamales M, Bonito-Oliva A, Herve D, Hoeffer C, Klann E, et al. Haloperidol regulates the state of phosphorylation of ribosomal protein S6 via activation of PKA and phosphorylation of DARPP-32. Neuropsychopharmacology : official publication of the American College of Neuropsychopharmacology. 2011; 36:2561–2570. [PubMed: 21814187]

Vauquelin G, Bostoen S, Vanderheyden P, Seeman P. Clozapine, atypical antipsychotics, and the benefits of fast-off D2 dopamine receptor antagonism. Naunyn-Schmiedeberg's archives of pharmacology. 2012; 385:337–372.

Witten IB, Lin SC, Brodsky M, Prakash R, Diester I, Anikeeva P, Gradinaru V, Ramakrishnan C, Deisseroth K. Cholinergic interneurons control local circuit activity and cocaine conditioning. Science. 2010; 330:1677–1681. [PubMed: 21164015]

Xiang Z, Thompson AD, Jones CK, Lindsley CW, Conn PJ. Roles of the M1 muscarinic acetylcholine receptor subtype in the regulation of basal ganglia function and implications for the treatment of Parkinson's disease. J Pharmacol Exp Ther. 2012; 340:595–603. [PubMed: 22135383]

Zeng XP, Le F, Richelson E. Muscarinic m4 receptor activation by some atypical antipsychotic drugs. European journal of pharmacology. 1997; 321:349–354. [PubMed: 9085047]

Zhang H, Sulzer D. Frequency-dependent modulation of dopamine release by nicotine. Nature neuroscience. 2004; 7:581–582. [PubMed: 15146187]

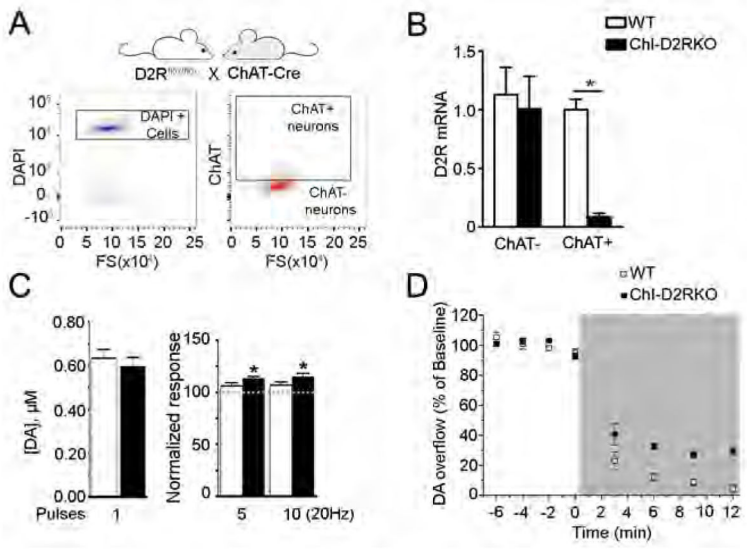

Figure 1. Characterization of ChI-D2RKO mice

A) Top: Cartoon of the mating strategy to obtain ChI-D2RKO mice. **Bottom**: FACS profiles of the DAPI positive cells (left) chosen for the sorting of ChAT positive (right) neurons. **B)** Quantifications of D2R mRNA expression (normalized to GAPDH) in qRT-PCR experiments of sorted striatal $ChAT^{-}$ and $ChAT^{+}$ cells from WT (white bar) and ChI-D2RKO mice (black bar) (n=3, $p<0.05$). **C)** Left: Cyclic voltammetry analysis of DA overflow by a single-pulse electrical stimulation (paired t-test, $p = 0.35$, $n = 30$). Right: train of 5 or 10 electrical stimulations (20 Hz) normalized to a preceding single pulse stimulation. The ChI-D2RKO mice show higher DA release probability than the WT (repeated measures 2-way ANOVA, genotype: $F_{(1,17)} = 12.81$, $p = 0.002$). **D)** DA overflow during quinpirole incubation at 0.5 µM. The ChI-D2RKO mice display a reduced quinpirole effect, as compared to WT, on the inhibition of DA overflow ($p < 0.001$, F test on nonlinear regression). All values are mean ± SEM, *$p<0.05$. See also Figure S1.

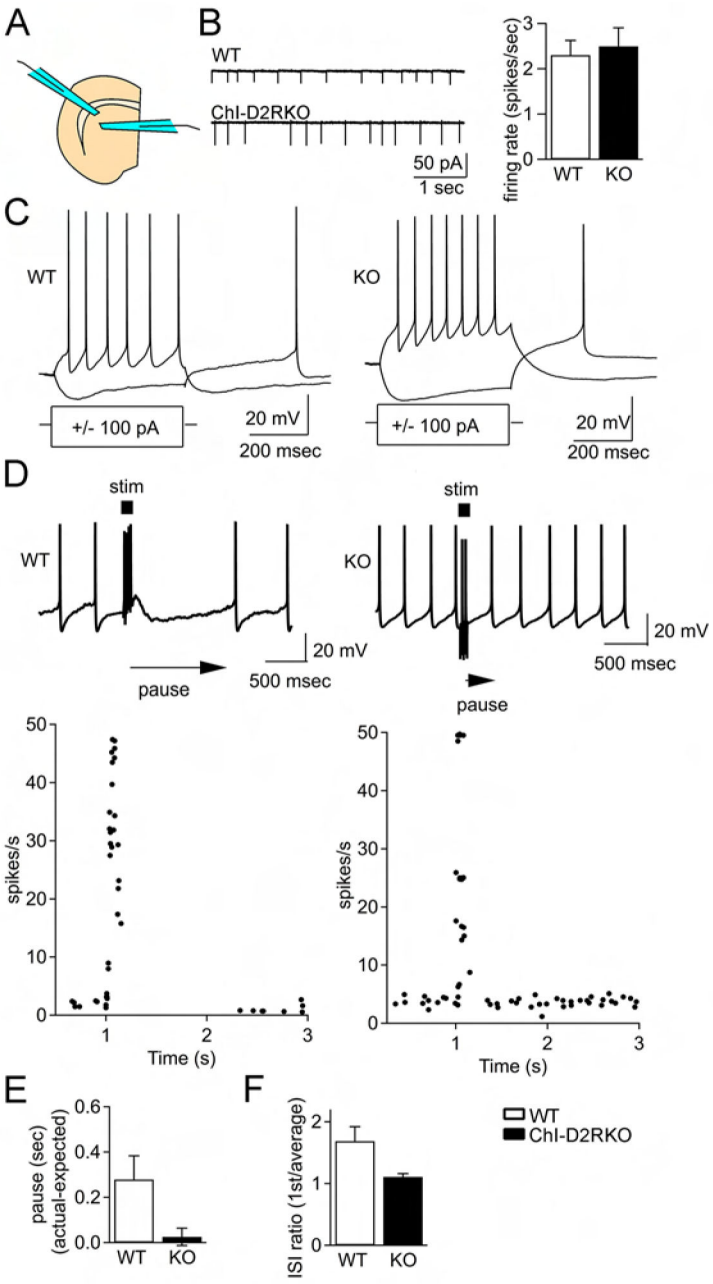

Figure 2. Reduction of the TAN "pause" in absence of D2R in ChI-D2RKO

A) Schematic diagram of the recording configuration showing a coronal slice containing the striatum, with stimulating and recording electrodes positioned in the dorsal striatum. Representative cell-attached recordings (in presence of picrotoxin) of ChIs from WT and ChI-D2RKO slices, each showing spontaneous action potential firing. **B)** Summary of average cell-attached firing rates in neurons from WT (n=15 neurons/N=6 mice) and ChI-D2RKO (n=13 neurons/N=5 mice) slices. **C)** Representative recording in whole-cell current-clamp mode, showing typical intrinsic properties of cholinergic interneurons, such as a hyperpolarization-activated current, or sag, rebound firing, and spike frequency adaptation to

depolarization in ChI-D2RKO and WT slices. **D)** Upper panels: Representative responses in ChI elicited by intrastriatal electrical stimulation (5 pulses delivered at 50 Hz). Cells were recorded in the whole-cell current-clamp configuration from WT (left) and ChI-D2RKO (right) slices, which fired additional action potentials in response to intrastriatal electrical stimulation. Lower panels: Summary of firing rate across multiple trials in the sample neurons, showing the firing rate before, during, and after each bout of intrastriatal stimulation. **E)** Summary of average pause in firing, expressed as the actual pause minus the expected pause (based on the interspike intervals in the pre-stimulation period), in WT (n=15 neurons/N=6 mice) and ChI-D2RKO (n=24 neurons/N=5 mice) slices. **F)** Summary of average pause, expressed as the ratio of the first interspike interval (ISI) to the average (pre-stimulation) interspike interval, in WT (n=15/N=6) and ChI-D2RKO (n=24/N=5) slices. See also Figure S2.

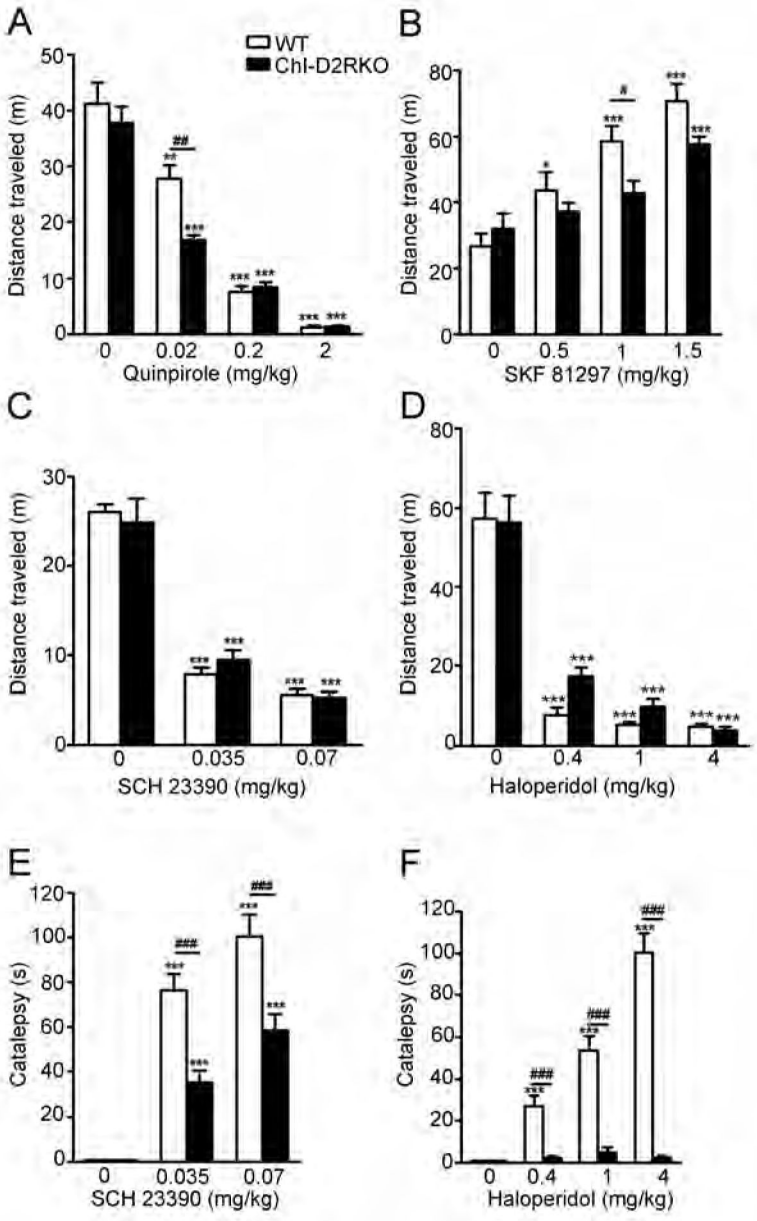

Figure 3. D2R on ChIs regulates motor activity and catalepsy in response to DA agonists and antagonists

A) Quinpirole-induced reduction of motor activity (30min) is accentuated in ChI-D2RKO at 0.02mg/kg as compared to WT mice (2-way ANOVA: genotype x treatment: $F_{(3,79)}$=3.17, p=0.029; genotype: $F_{(1,79)}$ =5.34, p=0.024; and treatment: $F_{(3,79)}$=143.8, p<0.0001). **B)** SKF81297-induced motor activity (1h) in ChI-D2RKO is significant only at 1.5mg/kg as compared to WT mice (2-way ANOVA: treatment: $F_{(3,59)}$= 24.8; p<0.0001 and genotype: F(1,59)= 6.5; p=0.013). All values are mean ± SEM. *P<0.05, **P<0.01, ***P<0.0001 vs saline; #p<0.05, ##p<0.01, ### p<0.001 between genotypes. **C)** SCH 23390 (15min) and **D)** haloperidol (1h) dose-dependently induced a similar reduction of motor activity in WT and ChI-D2RKO (2-way ANOVA: SCH 23390 treatment: $F_{(2,41)}$= 112.7; p<0.0001; haloperidol

treatment: $F_{(3,58)}$= 86.04; p<0.0001). **E)** SCH 23390-induced catalepsy (bar test; 30min after administration) is significantly reduced in ChI-D2RKO as compared to WT mice (2-way ANOVA: genotype x treatment: $F_{(2,36)}$ = 7.66; p=0.002, genotype $F_{(1,36)=}$ 31; p= 0.000 and treatment $F_{(2,36)}$ = 85.83; p=0.000). **F)** Absence of haloperidol-induced catalepsy in ChI-D2RKO mice (bar test; 1h after administration) in WT and ChI-D2RKO (2-way ANOVA: genotype x treatment: $F_{(3,53)}$ = 74.79; p=0.000; genotype $F_{(1,53)=}$ 336; p= 0.000 and treatment $F_{(3,53)}$ = 81.02; p=0.0001. All values are mean ± SEM. See also Figure S3.

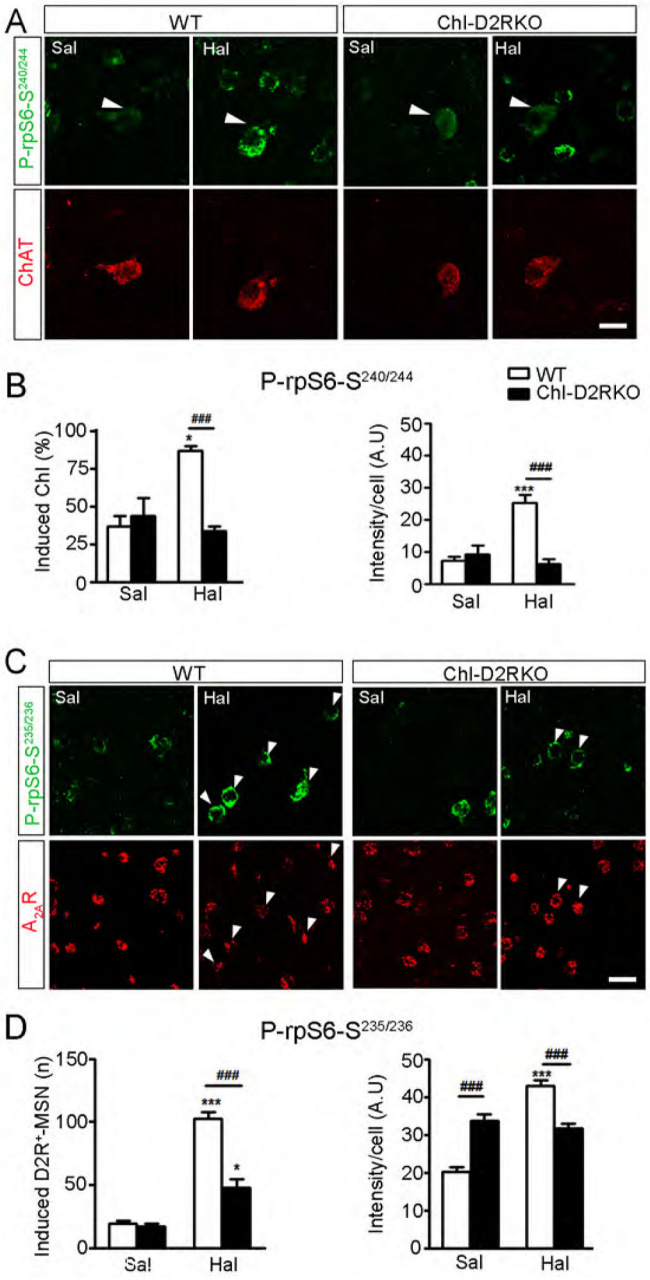

Figure 4. Dampened rpS6 signaling in ChI-D2RKO striata

A) Double immunofluorescence analyses of haloperidol-induced rpS6 phosphorylation in the DLS of WT and ChI-D2RKO ChIs using P-rpS6-$S^{240/244}$ and ChAT antibodies. Arrowheads indicate P-rpS6-$S^{240/244}$ labeling in $ChAT^{+}$ cholinergic interneurons. P-rpS6-$S^{240/244}$ induction is observed only in WT neurons. Scale bar: 20μm. **B)** Quantifications of experiments as shown in A) **Left**: rpS6-$S^{240/244}$ positive ChIs are observed only in WT but not in ChI-D2RKO sections (2-way ANOVA: genotype x treatment $F_{(1,11)}$ =17.05; p=0.003; genotype $F_{(1,11)}$=10.32, p=0.012 and treatment: $F_{(1,11)}$=7.58; p=0.025; and **Right**: the fluorescence intensity of P-rpS6-$S^{240/244}$/ChI after haloperidol increased only in WT but not

in ChI-D2RKO sections (2-way ANOVA: genotype x treatment: $F_{(1,11)}$ =23.59; p=0.001, genotype $F_{(1,11)}$=15.55, p=0.004 and treatment effect: $F_{(1,11)}$= 12.02, p=0.008) in haloperidol (Hal)-treated ChI-D2RKO vs WT sections **C)** Selective haloperidol-induced P-rpS6-$S^{235/236}$ in $A_{2A}R$ positive $D2R^+$-MSNs in the DLS of WT and ChI-D2RKO mice. Arrowheads point to $D2R^+$-MSNs showing the induction of P-rpS6-$S^{235/236}$ in $A_{2A}R^+$ neurons. Scale bar: 30μm. **D) Left**: Quantifications of experiments as shown in C) displaying significantly lower number of P-rpS6-$S^{235/236}$ and $A_{2A}R$ positive $D2R^+$-MSNs in ChI-D2RKO mice compared to WT (2-way ANOVA: genotype x treatment: $F_{(1,11)}$ =32.51, p=0.0005; genotype: $F_{(1, 11)}$=38.56, p=0.0003 and treatment effect: $F_{(1,11)}$= 152.68, p<0.0001). **Right**: Significant difference of P-rpS6-$S^{235/236}$ fluorescence intensity/$D2R^+$-MSN between WT and ChI-D2RKO sections (2-way ANOVA: genotype x treatment: $F_{(1,11)}$ =23.59; p=0.001; genotype: $F_{(1, 11)}$=15.55, p=0.004; treatment: $F_{(1,11)}$= 12.02, p=0.008). All values are mean ± SEM. Bonferroni's posthoc: ***p<0.001, *p<0.05 saline vs treated, ###p<0.0001, among genotypes. WT (white bars) and ChI-D2RKO mice (black bars).

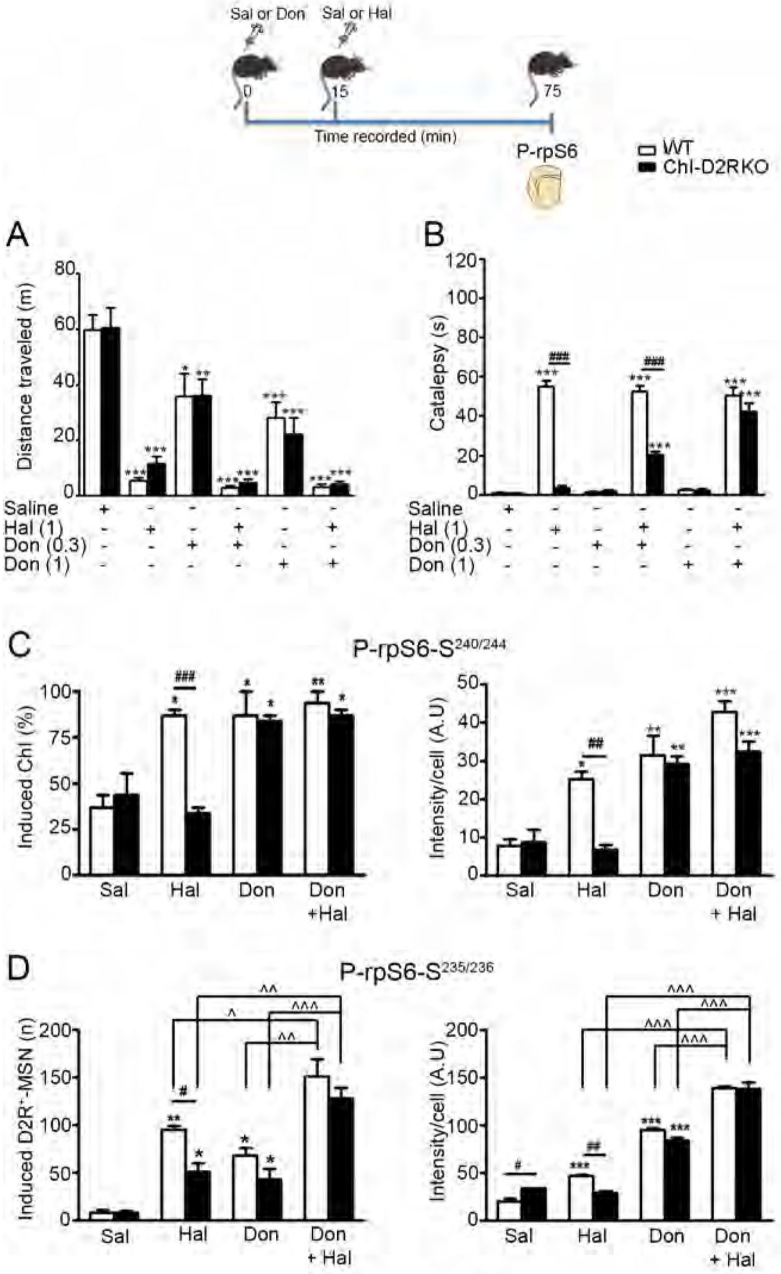

Figure 5. Donepezil rescues catalepsy in haloperidol treated ChI-D2RKO mice

Top: schematic of the experiment in A-D. **A)** Donepezil (Don; 1 and 0.3 mg/kg) and haloperidol (Hal: 1mg/kg) alone or combined, as indicated, equally affect motor activity in WT and ChI-D2RKO mice (2-way ANOVA: treatment $F_{(5, 93)}$=45.47, p<0.0001) and **B)** Donepezil partially (0.3mg/kg) or completely (1mg/kg) restores haloperidol-induced catalepsy in ChI-D2RKO mice (2-way ANOVA: treatment x genotype: $F_{(5,63)}$=28.42, p<0.0001, genotype $F_{(1,63)}$=87.27, p<0.0001 and treatment: $F_{(5,63)}$=109.79, p<0.0001); treatments are as indicated. **C)** Donepezil (1mg/kg) alone as well as combined to Hal (1mg/kg) restores rpS6-$S^{240/244}$ phosphorylation in the ChIs of ChI-D2RKO to WT levels.

Left: quantification of the percentage of P-rpS6-$S^{240/244}$ positive ChIs in WT and ChI-D2RKO mice upon treatment, as indicated (2-way ANOVA: treatment x genotype: $F_{(3,23)}$ =6.27, p=0.005; genotype $F_{(1,23)}$=7.05, p=0.017 and treatment: $F_{(3,23)}$=18.95, p<0.0001). **Right:** quantification of the fluorescence intensity of P-rpS6-$S^{240/244}$/ChI in WT and ChI-D2RKO mice (2-way ANOVA: treatment x genotype: $F_{(3,23)}$ =4.30, p=0.021; genotype $F_{(1,23)}$=12.75, p=0.002; treatment: $F_{(3,23)}$=40.65, p<0.0001). **D)** Combined effect of donepezil (1mg/kg) and haloperidol (1mg/kg) on P-rpS6-$S^{235/236}$ in D2R+-MSNs. **Left:** Quantification of the number of P-rpS6-$S^{235/236}$-positive $D2R^{+}$MSNs after treatment with donepezil (1mg/kg) and haloperidol (1mg/kg) alone or combined, as indicated (2-way ANOVA: genotype: $F_{(1, 23)}$=11.57, p=0.003 and treatment: $F_{(3,23)}$=65.45, p<0.0001). **Right:** quantification of the intensity of P-rpS6-$S^{235/236}$/$D2R^{+}$MSNs of both genotypes (2-way ANOVA: treatment x genotype: $F_{(3,23)}$=8.88, p=0.001 and treatment: $F_{(3,23)}$=497.03, p<0.0001). All values are mean ± SEM. *p<0.05, **p<0.01, ***p<0.0001 vs saline. #p<0.05, ##p<0.01, ### p<0.001 between genotypes, ^p<0.05, ^^ p<0.01, ^^^p<0.0001 between treatments. WT (white bars) and ChI-D2RKO mice (black bars). See also Figure S4.

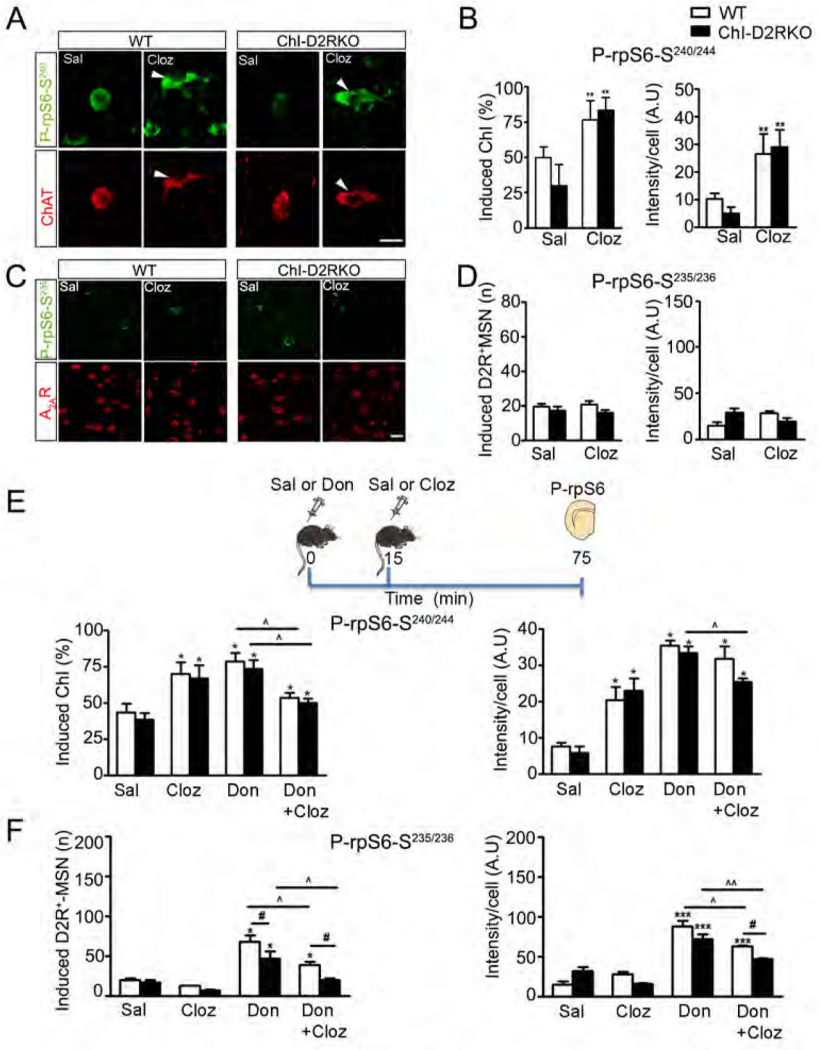

Figure 6. Similar clozapine-induced signaling in both genotypes

A–D) WT and ChI-D2RKO slices following clozapine (1mg/kg) or saline treatment, 1h after administration. **A)** Double immunostainings using P-rpS6-$S^{240/244}$ and ChAT (scale bar: 20 μm). Arrowheads point to $ChAT^{+}$ cholinergic interneurons showing P-rpS6-$S^{240/244}$ induction upon treatment. **B)** Quantifications of P-rpS6-$S^{240/244}$ positive ChI (left) (2-way ANOVA: treatment effect: $F_{(1,11)}$=16.32, p=0.0037) and of staining intensity/ChI (right) (2-way ANOVA: treatment effect: $F_{(1,11)}$=12.27, p=0.009). **C)** Double immunostainings using P-rpS6-$S^{235/236}$ and A2AR antibodies. Scale bar: 15 μm. **D)** Quantification of P-rpS6-$S^{235/236}$ and $A_{2A}R$ positive $D2R^{+}$MSNs (left) and of staining intensity/$D2R^{+}$MSN (right) (for both 2-way ANOVA showed no difference). **E)** Center: Schematic of the experiment. Quantifications of double immunofluorescence analyses of P-rpS6-$S^{240/244}$ in ChIs 1h after clozapine and donepezil alone or combined, as indicated. **Left:** percentage of P-rpS6-$S^{240/244}$ and ChAT positive ChIs (2-way ANOVA, treatment: $F_{(3,23)}$=13.79, p=0.0001). **Right:** quantification of P-rpS6-$S^{240/244}$ staining intensity/ChI (2-way ANOVA, treatment: $F_{(3,23)}$=48.41, p<0.0001). **F) Left:** quantification of number of P-rpS6$S^{235/236}$ and $A_{2A}R$

positive $D2R^+$-MSNs in sections treated as indicated (2-way ANOVA: genotype $F_{(1,23)}$=12.39, p=0.0028 and treatment: $F_{(3,23)}$=26.06, p<0.0001). **Right:** quantification of P-$S^{235/236}$rpS6 fluorescence intensity/$A_{2A}R^+$MSN (2-way ANOVA: treatment: $F_{(3,23)}$=12.17, p=0.0002). All values are mean ± SEM. *P<0.05, **P<0.01, ***P<0.0001 vs saline. #p<0.05, ##P<0.01, ### p<0.001. ^p<0.05, ^^ p<0.01, between treatments. WT (white bars) and ChI-D2RKO mice (black bars). See also Figure S5.

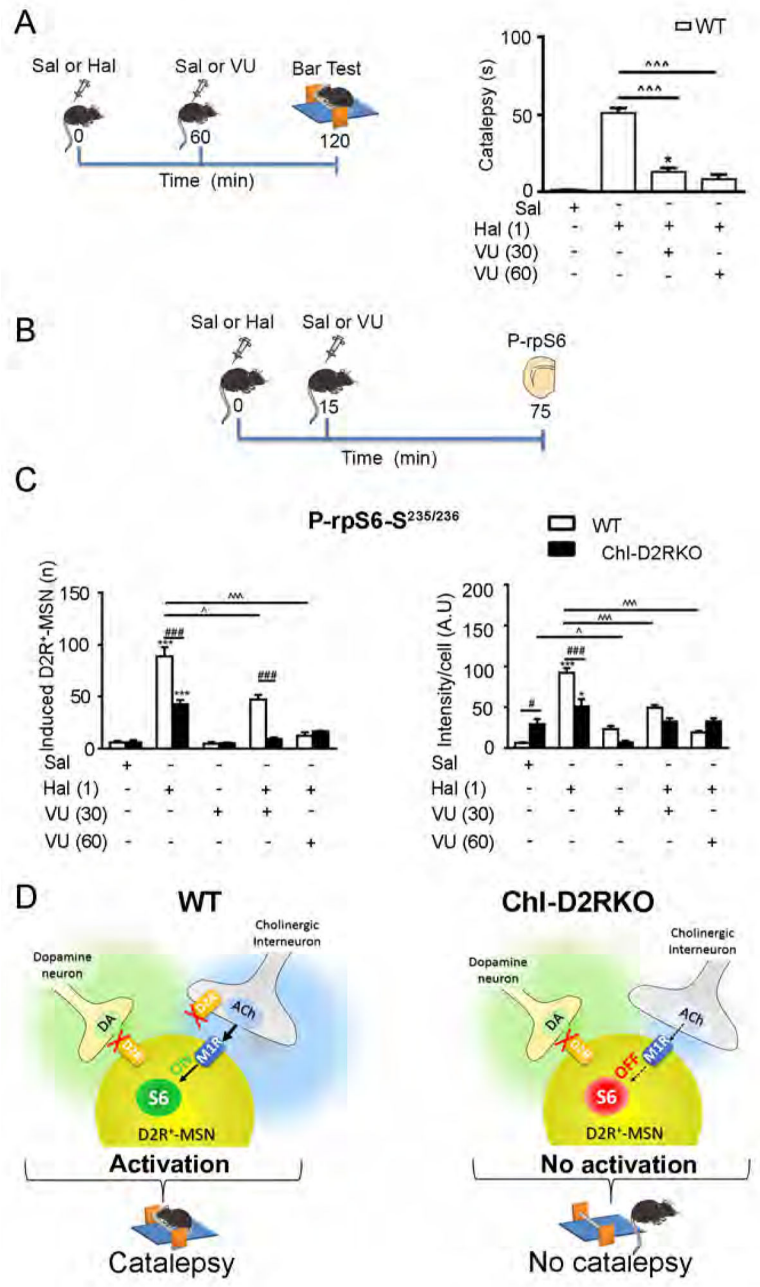

Figure 7. Blockade of muscarinic M1R prevents haloperidol-induced catalepsy

A) Left: Schematic of the experiment using haloperidol and VU0255035 alone or in combination as indicated. **Right:** VU0255035 prevents haloperidol-induced catalepsy in WT mice (1-way ANOVA: Treatment: $F_{(3,19)}=83.92$; $p<0.0001$. Bonferroni post-hoc test: *$p<0.05$ vs saline, ^^^ $p<0.001$ between treatments. **B)** Schematic of the experiment in C); **C)** Administration of VU0255035 in haloperidol treated mice abolishes rpS6-$S^{235/236}$ phosphorylation in D2R+-MSNs. **Left:** Quantification of the number of double labeled P-rpS6-$S^{235/236}$ and $A2AR^+$ $D2R^+$MSNs after haloperidol (1mg/kg) alone or combined with VU0255035 (30–60mg/kg), as indicated (2-way ANOVA: treatment x genotype: $F_{(4,25)}=23.22$, $p<0.0001$, genotype: $F_{(1, 25)}=49.44$, $p<0.0001$ and treatment: $F_{(4,25)}=100.4$,

p<0.0001) and **Right:** quantification of the intensity/cell of P-rpS6-$S^{235/236}$ staining in $A2AR^+$ $D2R^+$MSNs (2-way ANOVA: treatment x genotype: $F_{(4,25)}$=15.22, p<0.0001, genotype: $F_{(1,25)}$=6.49, p=0.0192 and treatment: $F_{(4,25)}$=48.82, p<0.0001). *p<0.05, ***p<0.0001 vs saline. ### p<0.001 between genotypes, ^p<0.05, ^^^p<0.0001 between treatments. WT (white bars) and ChI-D2RKO mice (black bars). All values are mean ± SEM. See also Figure S6. **D)** Model of haloperidol-induced catalepsy. **Left:** in WT mice, haloperidol (red cross) blocks the inhibitory D2R signaling on MSNs activating these neurons. Haloperidol also blocks D2Rs on ChIs increasing their activity (Bertran-Gonzalez et al., 2012) and ACh release. ACh acting through the muscarinic M1 receptor on $D2R^+$-MSNs and further activates these neurons. Thus, catalepsy is generated by the simultaneous activation of M1R and blockade of D2R in D2R+-MSNs. Absence of D2Rs in ChIs renders these neurons unresponsive to haloperidol. This results into decreased Ach signaling at M1R in $D2R^+$-MSNs and consequent lower stimulation of these neurons. Analyzing the levels of rpS6 phosphorylation monitors these changes. The final behavioral outcome is absence of catalepsy.